

Analytical solutions for Tokamak equilibria with reversed toroidal current

Caroline G. L. Martins,^{1,a)} M. Roberto,^{1,b)} I. L. Caldas,^{2,c)} and F. L. Braga^{1,d)}

¹*Departamento de Física, Instituto Tecnológico de Aeronáutica, São José dos Campos, São Paulo 12228-900, Brazil*

²*Instituto de Física, Universidade de São Paulo, 05315-970 São Paulo, SP, Brazil*

(Received 22 February 2011; accepted 22 July 2011; published online 19 August 2011)

In tokamaks, an advanced plasma confinement regime has been investigated with a central hollow electric current with negative density which gives rise to non-nested magnetic surfaces. We present analytical solutions for the magnetohydrodynamic equilibria of this regime in terms of non-orthogonal toroidal polar coordinates. These solutions are obtained for large aspect ratio tokamaks and they are valid for any kind of reversed hollow current density profiles. The zero order solution of the poloidal magnetic flux function describes nested toroidal magnetic surfaces with a magnetic axis displaced due to the toroidal geometry. The first order correction introduces a poloidal field asymmetry and, consequently, magnetic islands arise around the zero order surface with null poloidal magnetic flux gradient. An analytic expression for the magnetic island width is deduced in terms of the equilibrium parameters. We give examples of the equilibrium plasma profiles and islands obtained for a class of current density profile. © 2011 American Institute of Physics. [doi:10.1063/1.3624551]

I. INTRODUCTION

Plasmas are confined in tokamaks by magnetic field lines on nested axisymmetric toroidal magnetic surfaces.¹ This occurs for both conventional tokamaks, with an inductive plasma current density with a maximum at the centre,¹ and in tokamaks with a non-inductive current density with a maximum outside the centre, as presently in JET^{2,3} and predicted in the forthcoming ITER.⁴ However, some advanced confinement regimes with non inductive currents develop a radial hollow current profile, with a central hole where the current density is almost zero or even negative.⁵ The existence of stable current reversal equilibrium configurations is still subject of experimental investigation.⁵ Whenever a reversed current density is created, the magnetic surfaces are non-nested with magnetic islands since a magnetic field component normal to the average magnetic surface is generated.^{5,6} As this new configuration with current hole opens a new regime to be explored in tokamaks,⁵ it is useful to know solutions of the Grad-Shafranov equation¹ which describe magnetohydrodynamic (MHD) equilibria with non nested magnetic surfaces.

In Ref. 7, a negative current region in between the current hole and the external positive current region have been found possible only for isolated solutions, which do not depend continuously on the boundary and profile. However, after that, numerical or particular solutions for MHD equilibria with central negative current density have been found. In fact, in Ref. 8, a numerical solution for force-free equilibria with zero plasma pressure gradient was found, and in Ref. 9, an analytical solution of the Grad-Shafranov equation was obtained for a plasma equilibrium with a non uniform

pressure and a particular current profile. Moreover, a scheme to solve numerically the Grad-Shafranov equation with negative core toroidal current was presented in Ref. 10 and applied to experimental measurements from current hole discharges.¹¹ For a flux function in a quadratic polynomial form, numerical solutions of the Grad-Shafranov equation were obtained in Ref. 12 for tokamak equilibrium with reversed toroidal current.

In our work, we find analytical solutions, for the Grad-Shafranov equation, describing plasma equilibrium in a large aspect ratio tokamak for any kind of reversed hollow current density profiles. To obtain these solutions, in terms of non-orthogonal toroidal polar coordinates,¹³ we use a successive approximation method. These toroidal polar coordinates were introduced in previous works to evidence toroidal effects in the equilibrium field geometry.^{13,14}

For the considered reversed current profile, our zero order solution of the poloidal magnetic flux function depends only on the radial toroidal polar coordinate and describes nested toroidal magnetic surfaces with a singular surface where the flux gradient is null. The flux surfaces in a poloidal plane are not concentric circles but rather circles shifted toward the exterior equatorial region, as observed in every tokamak (the so called Shafranov shift¹). On the other hand, for the considered equilibrium with reversed current, the appearance of magnetic islands is related to our first order correction that depends on the radial and poloidal coordinates and introduces a magnetic field component normal to the zero order magnetic surface with a null flux gradient. In this framework, we also present an approximated analytical expression for the magnetic island width and show its dependence with the equilibrium parameters. Finally, we apply our results to a class of current density profile and present examples of the equilibrium plasma profiles and the predicted islands.

In Sec. II, we introduce the non-orthogonal toroidal polar coordinates and present the analytical solutions of the

^{a)}Electronic mail: carolinegameiro@gmail.com.

^{b)}Author to whom correspondence should be addressed. Electronic mail: marisar@ita.br.

^{c)}Electronic mail: ibere@if.usp.br.

^{d)}Electronic mail: leonciobraga@yahoo.com.br.

Grad-Shafranov equation. In Sec. III, we discuss our solutions for a chosen class of current density. Section IV is left to our conclusions.

II. ANALYTICAL EQUILIBRIUM MODEL

To describe the equilibrium magnetic field lines, we choose a coordinate system appropriated to the tokamak symmetry. We have used in this paper a polar toroidal non-orthogonal coordinate system $(r_t, \theta_t, \varphi_t)$ given by¹³

$$r_t = \frac{R_0^m}{\cosh \xi - \cos \omega}; \quad \theta_t = \pi - \omega; \quad \varphi_t = \varphi \quad (1)$$

in terms of the usual toroidal coordinates (ξ, ω, φ) , where R_0^m is the magnetic axis radius. They are related to the local coordinates (r, θ, φ) by the following relations:

$$r_t = r \left[1 - \frac{r}{R_0^m} \cos(\theta) + \left(\frac{r}{2R_0^m} \right)^2 \right]^{1/2}, \quad (2)$$

$$\sin(\theta_t) = \sin(\theta) \left[1 - \frac{r}{R_0^m} \cos(\theta) + \left(\frac{r}{2R_0^m} \right)^2 \right]^{-1/2}. \quad (3)$$

In the large aspect ratio limit ($r_t \ll R_0^m$), r_t and θ_t become r and θ , respectively.¹³

Fig. 1 shows some coordinate surfaces of the $(r_t, \theta_t, \varphi_t)$ system. Note that the $r_t = \text{const}$, curves have a pronounced curvature in the interior region of the torus, from where we start counting poloidal θ_t angles. It is worthwhile to comment that for the so-called local coordinates (r, θ, φ) , that are a kind of cylindrical coordinates with toroidal curvature, the coordinate surfaces $r = \text{const}$ does not coincide with actual equilibrium magnetic surfaces. In contrast to that, as we show later on, one of the main advantages of using the to-

roidal helical coordinates is that the condition $r_t = \text{const}$ gives the toroidal magnetic surfaces already in the zero order approximation. Moreover, the origins of these two coordinate systems are the magnetic axis.

Finally, the relation of the magnetic axis radius R_0^m with the coordinate R is

$$R^2 = R_0^{m2} \left[1 - 2 \frac{r_t}{R_0^m} \cos \theta_t - \left(\frac{r_t}{R_0^m} \right)^2 \sin^2 \theta_t \right]. \quad (4)$$

The equilibrium magnetic fields in tokamaks can be obtained from MHD equilibrium theory. The equilibrium magnetic field lines lie on constant pressure surfaces or magnetic surfaces. This property can be described by a scalar function, a surface quantity ψ , such as $B_0 \cdot \nabla_p = 0$, where B_0 is the plasma equilibrium magnetic field and the magnetic surfaces are characterized by $\psi = \text{constant}$.¹³ The tokamak equilibrium magnetic field B_0 is obtained from an analytical solution of the Grad-Shafranov equation in these coordinates,¹³ such as $\psi = \psi(r_t, \theta_t)$. Besides, the intersections of the flux surfaces $\psi_p = \text{constant}$ with a toroidal plane are not concentric circles but rather present a Shafranov shift toward the exterior equatorial region.¹³

For large aspect-ratio and almost circular sections, the solution for the Grad-Shafranov equation can be written in terms of the toroidal coordinates as^{13,14}

$$\psi(r_t, \theta_t) = \psi_0(r_t) + \psi_1(r_t, \theta_t), \quad (5)$$

where $\psi_0(r_t)$ and $\psi_1(r_t, \theta_t)$ are the zero and the first order solutions of the poloidal magnetic flux, respectively.

The zero order solution can be obtained from the equation^{13,14}

$$\frac{1}{r_t} \frac{d}{dr_t} \left(r_t \frac{d\psi_0}{dr_t} \right) = \mu_0 J_\varphi(r_t), \quad (6)$$

where J_φ is the zero order toroidal component of the equilibrium plasma current density, which is a function of r_t coordinate. In this approximation, J_φ and the zero order pressure P_0 are related by

$$-(R_0^m)^2 \frac{dP_0}{d\psi_0}(\psi_0) = \beta_p J_\varphi(\psi_0). \quad (7)$$

Thus, in the zero order approximation only the coordinate r_t appears in Eq. (6) and $\psi_0(r_t)$ can be easily obtained in a closed-form/quadrature for any chosen current density profile. Moreover, Eq. (6) is identical to the Grad-Shafranov equation for a straight cylindrical plasma except for the definition of the coordinates. The zero order toroidal current dependence only on $\psi_0(r_t)$ is a property of the special coordinates used in our model.

The first order term (in the used toroidal polar coordinates) of the poloidal magnetic flux depends on r_t , and θ_t gives the asymmetry of the poloidal magnetic field in the equatorial plane.¹³ A successive approximation method was used in Ref. 13 to obtain the first order solution, which can be written as

$$\psi_1(r_t, \theta_t) = \frac{a}{R_0} f(r_t) \psi_0' \cos(\theta_t), \quad (8)$$

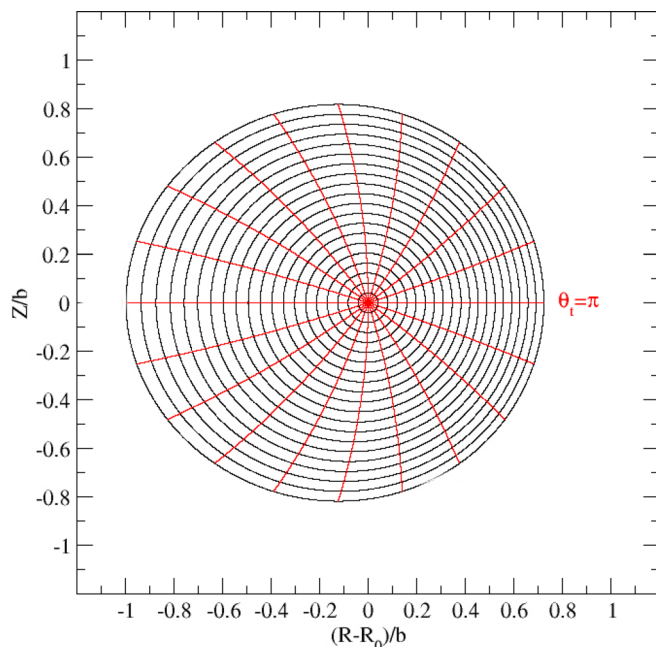


FIG. 1. (Color online) Some coordinate surfaces of the polar toroidal coordinate system in the $\varphi = 0$ plane.

where the prime denotes the derivative with respect to r_t and a is the plasma radius. It is shown in Ref. 13 that there is a solution for Eq. (8) for f depending on r_t only

$$\frac{df}{dr_t} \approx \frac{1}{a} \left[(1 - \beta_p) r_t - \frac{1}{r_t \psi_0'^2} \int_0^{r_t} \rho \psi_0'^2(\rho) d\rho \right]. \quad (9)$$

Here β_p is the ratio between thermal kinetic pressure and magnetic pressure. The integral on the right side of Eq. (9) can be expressed by

$$\int_0^{r_t} \rho \psi_0'^2(\rho) d\rho = \frac{r_t^2 \psi_0'^2}{2} - \int_0^{r_t} \psi_0' \psi_0'' \rho^2 d\rho. \quad (10)$$

To simplify the next expressions and obtain a short analytical solution for the poloidal flux function, we neglect the second term in Eq. (10) that is several orders of magnitude smaller than the first term. Physically, this means that the internal inductance per unit length in this case is $l_i \approx 1$. Considering the boundary condition $\psi(r_t = 0, \theta_t) = 0$, the flux function can be approximated by

$$\psi(r_t, \theta_t) \approx \psi_0(r_t) + \psi_0' \cos(\theta_t) \frac{(1 - 2\beta_p)}{4R_0} r_t^2. \quad (11)$$

To solve the Grad-Shafranov equation, we give the zero order profiles of current density J_ϕ and the poloidal current function I (I is a constant in the zero order approximation).

The equilibrium magnetic field components, in terms of the surface functions ψ and I , are

$$B_{r_t} = -\frac{1}{R_0^m r_t} \frac{\partial \psi(r_t, \theta_t)}{\partial \theta_t}, \quad (12)$$

$$B_{\theta_t} = -\frac{1}{R_0^m r_t} \frac{\partial \psi(r_t, \theta_t)}{\partial r_t}, \quad (13)$$

$$B_{\phi_t} = \frac{\mu_0 I_e}{2\pi (R_0^m)^2} \left[1 - 2 \frac{r_t \cos(\theta_t)}{R_0^m} \right]^{-1}. \quad (14)$$

To obtain Eq. (14), we consider the poloidal current function (the current density flux through the same surface used in the definition of ψ) in the large aspect ratio limit and in this case $I \approx -I_e/2\pi$ [Ref. 14], where I_e is the external current that generates the equilibrium toroidal field.

The safety factor $q(r_t)$ is defined as an average in θ_t so that

$$q(r_t) = \frac{1}{2\pi} \int_0^{2\pi} \left| \frac{B_{\phi_t}}{B_{\theta_t}} \right| d\theta_t, \quad (15)$$

which describes the field line helicity and diverges at $r_t = r_{ts}$.

For the reversed current profile considered in this work, the zero order solution, $\psi_0(r_t)$ of the poloidal magnetic flux function depends only on the toroidal polar radial coordinate, r_t , and describes nested toroidal magnetic surfaces with a surface where $\nabla \psi_0(r_t = r_{ts}) = 0$. This dependence of ψ_0 on the coordinate r_t means that the topology of the flux surfaces with $\psi_0(r_t) = \text{constant}$, in a poloidal plane, are not concentric circles but rather circles shifted toward the exterior equa-

torial region, as observed in every tokamak (the so called Shafranov shift¹). Thus, the solution $\psi_0(r_t)$ already contains some of the usual first order correction in the local polar coordinates, as the Shafranov displacement.

On the other hand, the appearance of magnetic islands is related to the first order correction, $\psi_1(r_t, \theta_t)$, that depends on the radial and poloidal coordinates and introduces a magnetic field component normal to the zero order magnetic surface in $r_t = r_{ts}$. Consequently, the considered large-aspect ratio equilibrium with almost concentric circular surface sections¹³ has two magnetic islands.

III. PROPOSED CURRENT DENSITY MODEL: RESULTS AND DISCUSSIONS

As an example, we consider the following non-monotonic zero order current density profile with a central hollow and a peak outside the center. This profile has two parameters and can represent well, at least qualitatively, the kind of expected profiles in the literature.⁶

$$J_\phi(r_t) = \frac{I_p R_0^m (\gamma + 2)(\gamma + 1)}{\pi a^2 (\beta + \gamma + 2)} \left[1 + \beta \left(\frac{r_t}{a} \right)^2 \right] \left[1 - \left(\frac{r_t}{a} \right)^2 \right]^\gamma. \quad (16)$$

Here I_p is the plasma current, β and γ are free parameters chosen to fit the desired reversed current profile, where $\gamma > 0$ and $\beta < 0$.

As the zero order solution is θ_t independent, the first derivative of flux function can be expressed by

$$\frac{d\psi_0}{dr_t} = \frac{\mu_0 I_p R_0^m}{2\pi r_t} \left[1 - \left(1 + \beta' \frac{r_t^2}{a^2} \right) \left(1 - \frac{r_t^2}{a^2} \right)^{\gamma+1} \right], \quad (17)$$

where $\beta' = \beta(\gamma + 1)/(\beta + \gamma + 2)$.

The corresponding explicit expression for the safety factor is

$$q(r_t) = q(a) \frac{r_t^2}{a^2} \left[1 - \left(1 + \beta' \frac{r_t^2}{a^2} \right) \left(1 - \frac{r_t^2}{a^2} \right)^{\gamma+1} \right]^{-1} \times \left(1 - 4 \left(\frac{r_t}{R_0^m} \right)^2 \right)^{-1/2}, \quad (18)$$

where

$$q(a) = \frac{I_e a^2}{I_p R_0^m}. \quad (19)$$

To obtain the figures presented in this work, we choose $q(a) \approx 5$.

To complement the equilibrium description, the pressure profile can be obtained from Ref. 7. Besides, in the considered coordinate system and in the large aspect ratio limit, the diamagnetic term does not contribute to the zero order (see Eq. (7)). The main contribution of the first order is to break the zero order symmetry and creates an island chain located at the singular magnetic surface (with a null flux gradient).

In Figs. 2(a) and 2(b), we present the radial profiles of the reversed toroidal current density, the poloidal magnetic

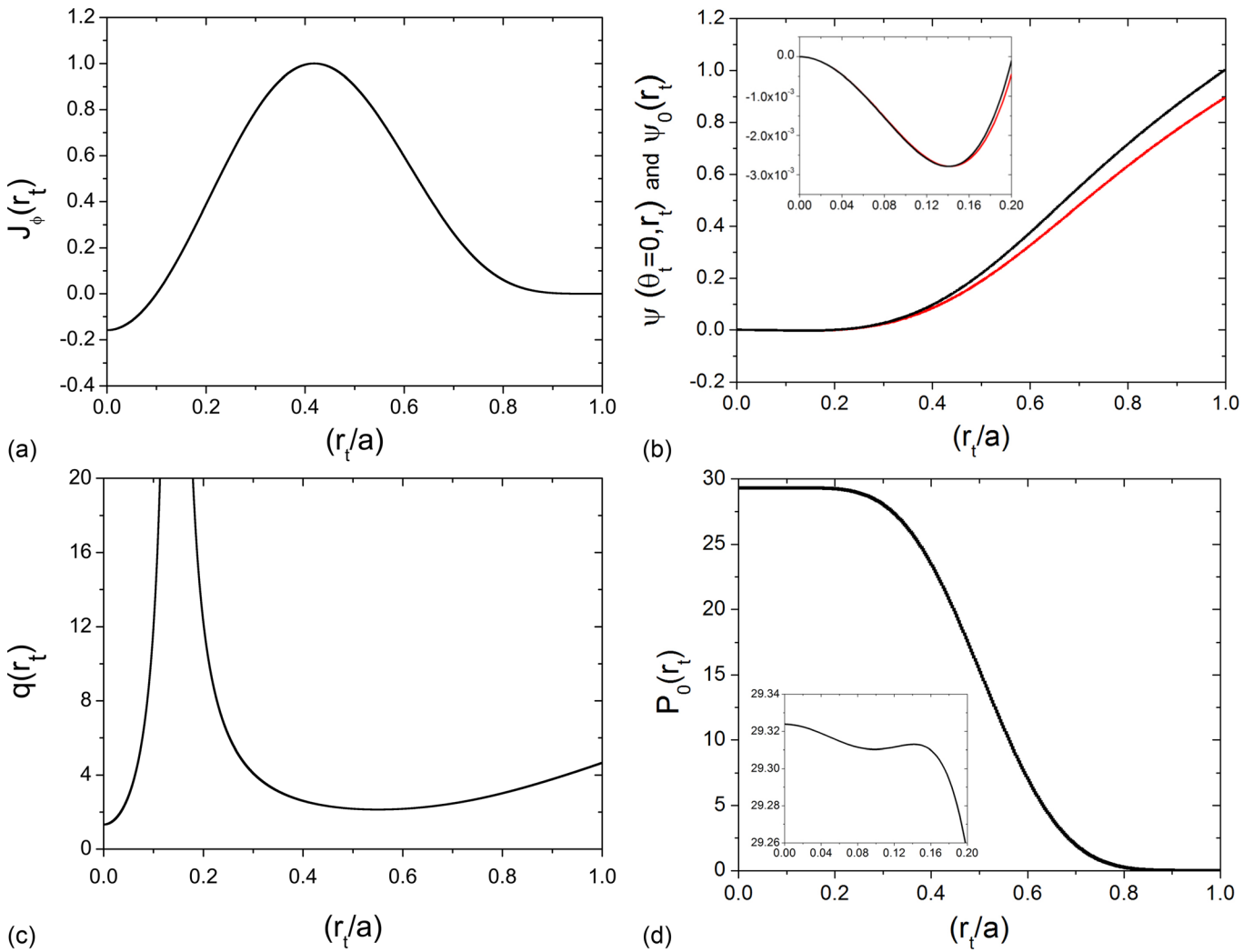


FIG. 2. (Color online) Parameters $\gamma = 5.0$, $\beta = -100.20$, and $\beta_p = 0.2$. (a) Toroidal current density normalized to its maximum value, $J_{\phi 0}(r_t)$; (b) poloidal magnetic fluxes normalized to their maximum values. $\Psi(\theta_t = 0, r_t)$ and $\Psi_0(r_t)$ are the flux with the first order correction (in black) and the zero order flux (in red), respectively; (c) zero order safety factor for the nested surfaces in radial intervals without islands; (d) pressure, $P_0(r_t)$, normalized to $\frac{\mu_0 I_p^2}{\pi a^2}$.

flux function normalized to their maximum values, respectively, for a set of parameters $\gamma = 5.0$, $\beta = -100.20$, $\beta_p = 0.2$, as a function of (r_t/a) . In this case, $\psi'_0(r_t) = 0$ for $r_t = 0$ and $r_{ts} = 0.142a$. We also choose $(a/R_0^m) = 0.29$, which is a typical value for tokamaks.¹⁵ In Fig. 2(b), the zero order solution of the Grad-Shafranov equation is represented by the red curve and the black curve gives the solution with the first order correction. As expected, the first order correction is almost negligible compared to the zero order approximation. In Fig. 2(c), we show the zero order safety factor profile calculated for nested surfaces.

Figure 2(d) shows the approximated pressure profile estimated from Eq. (7). The radial pressure profile is almost flat in the plasma center and decreases to the border as required for a good confinement. In general, for the non monotonic current density, the zero order pressure and other so-called flux functions are no longer strictly defined functions but become multi-valued applications of ψ_0 . Thus, the same value of ψ_0 may correspond to two different values of pressure, but still so, the pressure is constant over a given flux surface with a constant value of ψ_0 . This can be seen for

the amplified zero order pressure profiles of Figs. 2(d) and 5(b). Furthermore, as pointed in Ref. 10, the pressure $P(\psi)$ cannot be monotonic as its derivative changes sign when crossing the singular surface. In our procedure, even the first order correction would also be non monotonic because it is determined by the second derivative of pressure with respect to ψ_0 [Ref. 13].

In Fig. 3, we consider the flux function corrected up to the first order, as given by Eq. (11). Figure 3(a) shows in black the magnetic surface intersections with a fixed poloidal plane, obtained by using Eq. (11), while the colors represent the poloidal magnetic field values. Thus, this figure indicates the poloidal magnetic shear, where the change from cyan to light green indicates the transition from negative to positive values of the poloidal magnetic field. Two magnetic islands arise in the region where $B_{\theta t}(r_t = r_{ts}) = 0$. Fig. 3(b) shows, in the plane $r_t \times \theta_t$, a better view of the same island chain and its separatrix. The separatrix is formed by the superposition of two lines. One is the $r_t = r_{ts}$ line since the first order correction $\psi_1 = 0$ at this radial position. The other line will be

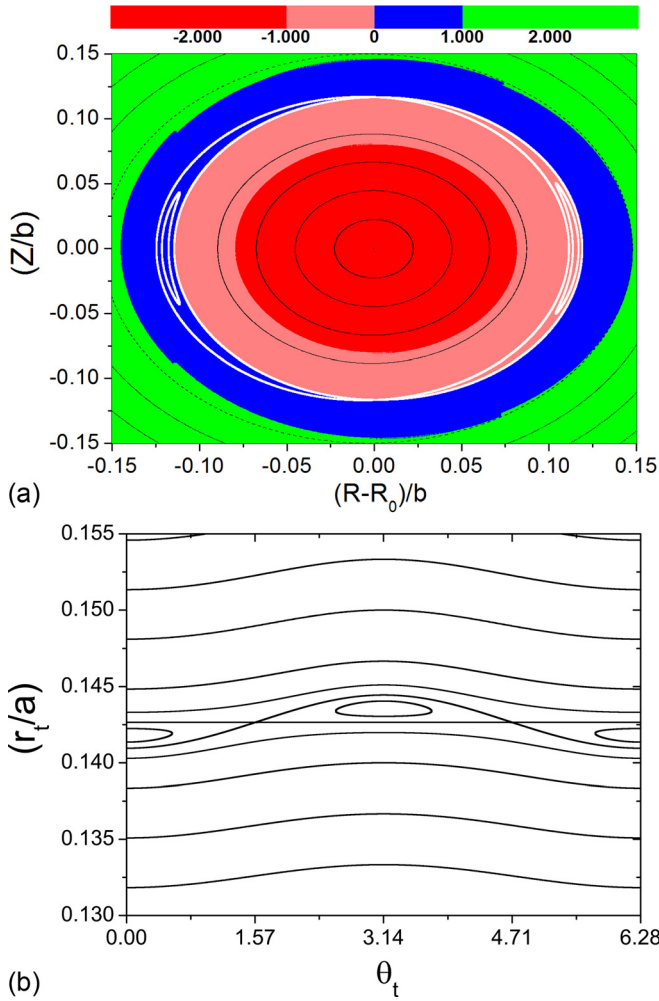


FIG. 3. (Color online) Parameters $\gamma = 5.0$, $\beta = -100.20$, and $\beta_p = 0.2$. (a) Color polar map of poloidal magnetic field, $B_{\theta}(r_t)$, and magnetic surfaces (in black); (b) The same magnetic surfaces and islands of (a) in the plane (r_t, θ_t) .

derived in the following paragraph. As we considered equilibria with almost circular sections, we always find two islands, as it can be verified in the expansion of

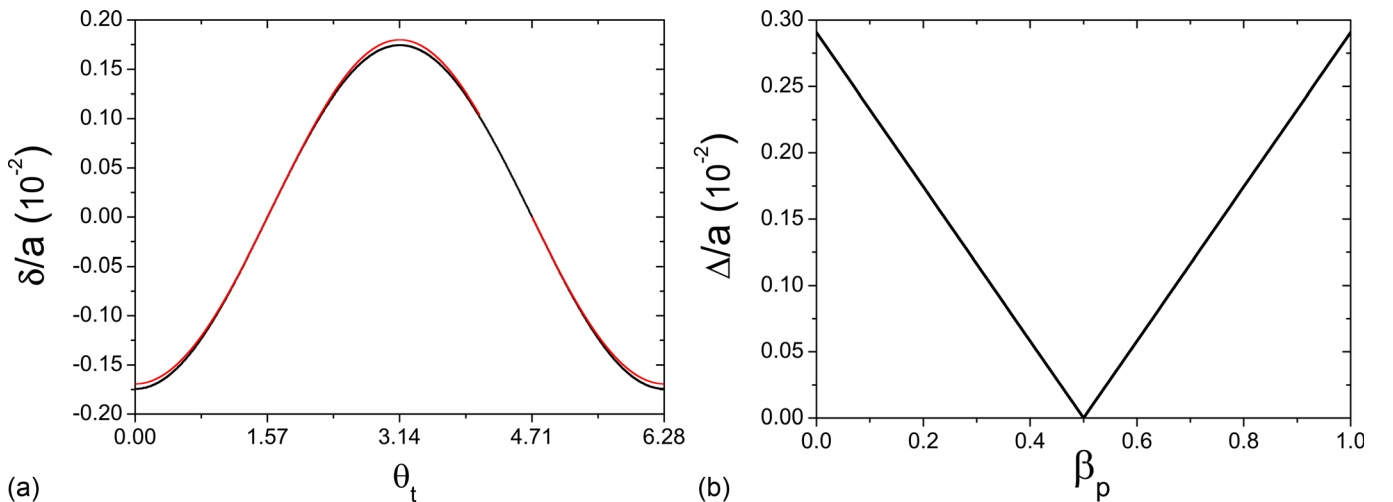


FIG. 4. (a) (Color online) Island separatrixes for $\beta_p = 0.2$. The black and red curves were obtained, respectively, by Eq. (22) and numerically from Fig. 3(b) and (b) dependence of magnetic islands width with β_p , obtained from Eq. (23).

Eq. (20), which gives in Eq. (21), a term in $\cos\theta$. Solutions with other plasma sections would present a different number of islands.⁹ Analytical solutions for non circular plasma sections could be searched introducing a θ_t dependence on the flux function ψ and would require the solution of a modified Eq. (6) with derivative of ψ with respect to the variable θ_t .

To determine the separatrix and the magnetic island width dependence on the confinement parameters, we perform a Taylor series expansion of the poloidal magnetic flux around $r_t = r_{ts}$. This expansion has some peculiarities due to the considered reversed current density. Namely, we consider the expansion for $\psi_0(r_t)$ up to the second order approximation and the expansion for $\psi_1(r_t, \theta_t)$ up to the first order approximation, since we have $|\psi_1(r_t, \theta_t)/\psi_0(r_t)| \ll 1$ and $\psi_1(r_{ts}) = 0$. Thus, following this expansion, we obtain

$$\psi(r_t, \theta_t) \approx \psi_0(r_{ts}) + \psi_1(r_{ts}, \theta_t) + \left[\frac{\partial \psi_0(r_t)}{\partial r_t} \Big|_{r_{ts}} + \frac{\partial \psi_1(r_t, \theta_t)}{\partial r_t} \Big|_{r_{ts}} \right] \times (r_t - r_{ts}) + \left[\frac{\partial^2 \psi_0(r_t)}{\partial r_t^2} \Big|_{r_{ts}} \right] \frac{(r_t - r_{ts})^2}{2} + O^3. \quad (20)$$

Since $\psi_1(r_{ts}, \theta_t) = 0$ and $\frac{\partial^2 \psi_0(r_t)}{\partial r_t^2} \Big|_{r_{ts}} = \mu_0 J_\phi(r_{ts})$, we introduce $\delta = (r_t - r_{ts})$ and obtain the following expression:

$$\delta \approx \frac{-2 \left[\frac{\partial \psi_1(r_t, \theta_t)}{\partial r_t} \Big|_{r_{ts}} \right]}{[\mu_0 J_\phi(r_{ts})]} \approx \frac{-\cos(\theta_t)(1 - 2\beta_p)r_{ts}^2}{2R_0^m}. \quad (21)$$

We point out that for the considered equilibrium, we have only one solution for the separatrix equation corresponding to the curve observed in Fig. 4(a), in contrast to the two usual solutions found for other approximated expressions derived for islands caused by resonant perturbations. This solution gives one separatrix side, the other side is the line $r_t = r_{ts}$ once, for the considered equilibrium, $\psi_1(r_{ts}) = 0$.

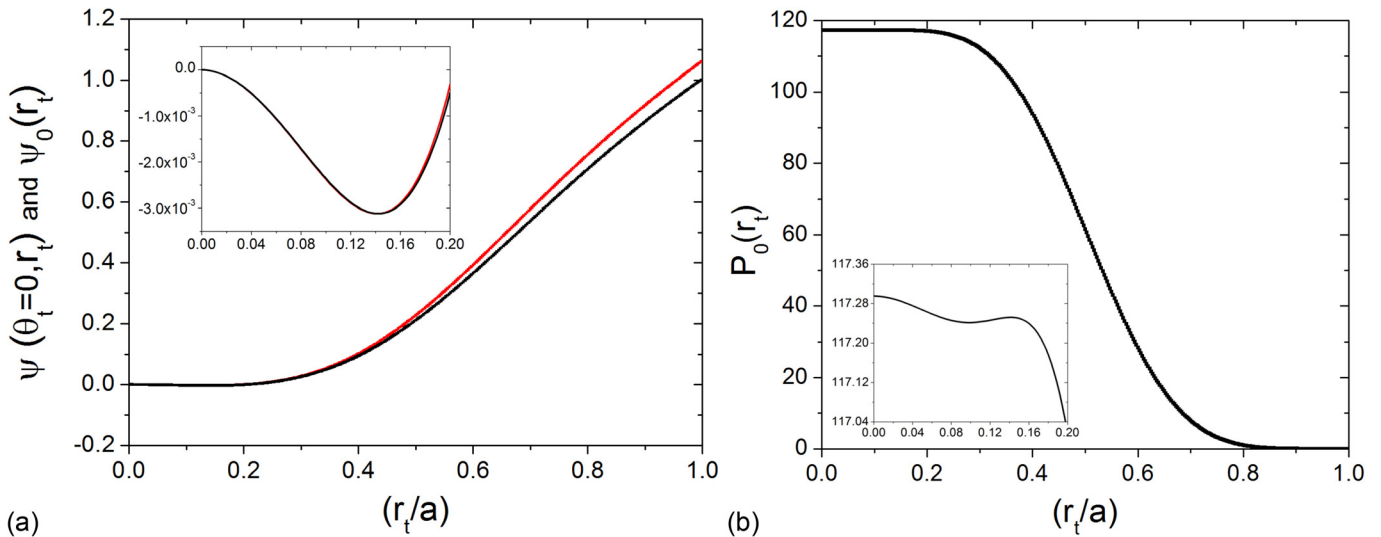


FIG. 5. (Color online) Parameters $\gamma = 5.0$, $\beta = -100.20$, and $\beta_p = 0.8$. (a) Poloidal magnetic fluxes normalized to their maximum values. $\Psi(\theta_t = 0, r_t)$ and $\Psi_0(r_t)$ are the flux with the first order correction (in black) and the zero order flux (in red), respectively and (b) normalized pressure, $P_0(r_t)$.

Equation (21) gives an approximated analytical expression for points located at the second separatrix component of the hyperbolic fixed points that create the islands. Fig. 4(a) shows the island separatrices obtained by using Eq. (21) (black curve) and the exact one (red curve) obtained numerically from Fig. 3(b). We obtain from Eq. (21) the width for the island located at $\theta_t = \pi$

$$\Delta \approx \left| \frac{(1 - 2\beta_p)r_{ts}^2}{2R_0^m} \right|. \quad (22)$$

This approximated analytical expression for magnetic island width depends on three numerical values: the singular magnetic surface radius r_{ts} , where $B_{\theta t}(r_{ts}) = 0$, the magnetic major axis radius R_0^m , and the ratio between the average thermal kinetic pressure and the poloidal magnetic pressure, β_p . In addition, the r_{ts} value is determined by the parameters γ and β that appear in Eq. (16).

For a fixed parameter R_0^m , we can see in Fig. 4(b) the values of the island width obtained from Eq. (22) as a function of the parameter β_p . The width decreases with β_p until $\beta_p = 0.5$ and after that the width of the island increases. For $\beta_p = 0.5$, the island disappears due to the absence of an asymmetry poloidal field. Thus, for symmetric poloidal magnetic field radial profiles, magnetic islands will not be formed even for strongly reversed toroidal current.

Now, we consider another equilibrium with a higher poloidal beta, namely, $\beta_p = 0.8$. The parameters $\gamma = 5.0$ and $\beta = -100.20$ are the same considered in the first equilibrium, such that the current density profile and, consequently, the singular magnetic surface radius is the same, $r_{ts} = 0.142a$. We also keep $(a/R_0^m) = 0.29$. For these parameters, Fig. 5(a) shows the radial profile of the poloidal magnetic flux function normalized to its maximum values. In Fig. 5(a), the zero order solution of the Grad-Shafranov equation is represented by the red curve and the black curve gives the solution with the first order correction. As expected, the first order correction is

almost negligible compared to the zero order approximation. As predicted by Eq. (11), in the second equilibrium (with a high poloidal beta), the first order correction increases the flux function, contrary to the decrease observed in Fig. 2(b) for the first equilibrium (with a low poloidal beta). In Fig. 5(b), we present the pressure profile obtained from Eq. (7). The pressure radial profile is similar to that shown in Fig. 2(d) for the first equilibrium, but the pressure values are higher for the second equilibrium as expected for high beta poloidal case. The safety factor profile is not shown in this case because it is similar to the one shown in Fig. 2(c).

We present in Fig. 6 the islands for the second equilibrium. We notice in Fig. 6(a) that the two islands appear in different positions compared to Fig. 3(a) for the previous equilibrium. This inverted position occurs for $\beta_p > 0.5$ (after the island vanishing for $\beta_p = 0.5$). Fig. 6(b) shows, in the plane $r_t \times \theta_t$, a better view of the same island chain and its separatrix. Fig. 6(c) shows the island separatrices obtained by using Eq. (21) (black curve) and the exact one (red curve) obtained numerically from Fig. 6(b). The islands are inverted when compared to Fig. 4(a). Finally, we mention that the island widths are the same for the two considered equilibria.

In this section, to give examples of our analytical method to solve the Grad-Shafranov equation, we choose equilibria with different parameters and show plasma profiles obtained from the considered current density. The results presented in the figures show that our zero order solutions describe very well the radial profile. Although our first order corrections do not change much the radial profiles, they are relevant because they introduce a poloidal angular dependence on these profiles. Our results show how this angular dependence generates the non-nested magnetic surfaces with islands on the singular surface. The considered examples show that our analytical solutions are adequate for further analysis to determine the plasma parameter influence on any MHD equilibrium property.

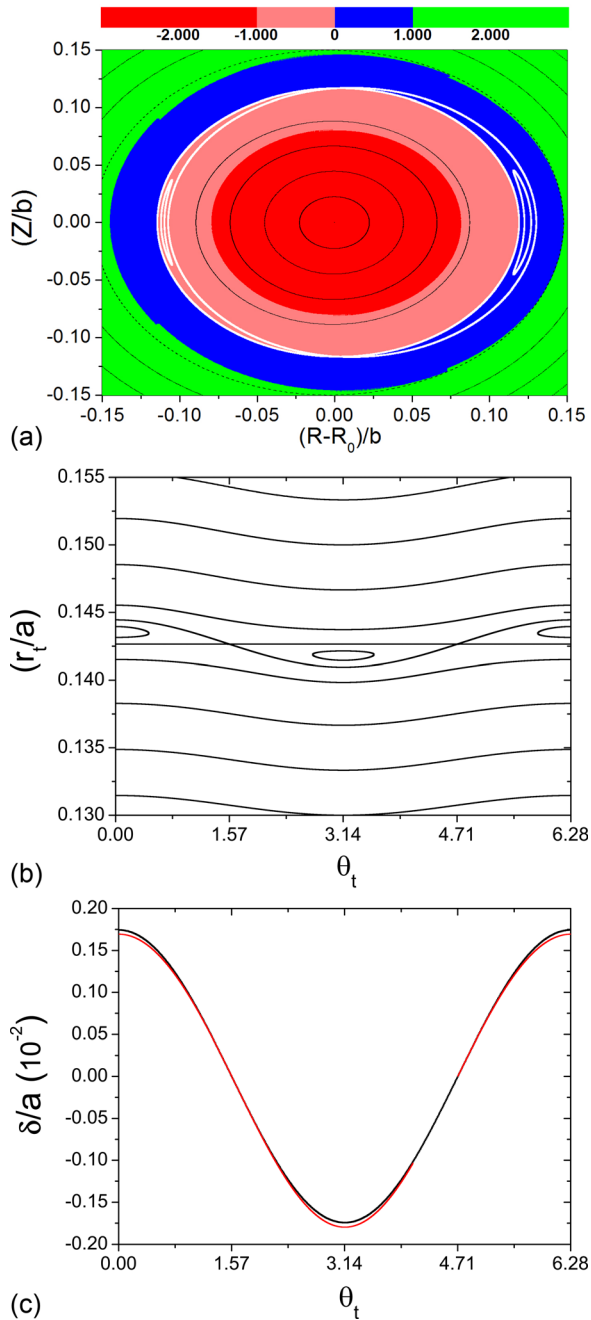


FIG. 6. (Color online) Parameters $\gamma = 5.0$, $\beta = -100.20$, and $\beta_p = 0.8$. (a) Color polar map of poloidal magnetic field, $B_{\theta}(r_t)$, and magnetic surfaces (in black); (b) the same magnetic surfaces and islands of (a) in the plane (r_t, θ_t) ; and (c) Island separatrixes. The black and red curves were obtained, respectively, by Eq. (22) and numerically from (b).

IV. CONCLUSIONS

In conclusion, we obtained an analytical solution of the Grad-Shafranov equation in terms of non-orthogonal toroidal polar coordinates for a reversed toroidal current profile that generates magnetic islands inside the plasma column. In our approach, the zero order solution described nested toroidal magnetic surfaces with a singular surface with null poloidal magnetic flux gradient, i.e., null poloidal magnetic field. The first order correction introduced in the magnetic flux a poloidal angular dependence and gave rise to two islands around

the surface with a null poloidal magnetic field. For the first time, an approximated analytical expression for the magnetic island width was deduced for an arbitrary reversed current profile. Thus, for a fixed magnetic axis radius, we found that the islands width was determined by the average poloidal beta and the radial position where the poloidal magnetic field vanishes. Furthermore, we applied our results for a low and a high poloidal beta equilibria.

Despite the relevant published papers addressing the reversed MHD equilibria numerically or analytically for particular plasma profiles, in the literature there are not yet analytical solutions for the Grad-Shafranov equation for the equilibria considered in this article. So, our approximated solution for almost circular plasma sections is already a significant contribution that could be used in further equilibrium and transport investigations to understand the discussed equilibria. Other analytical solutions for non circular plasma sections could be searched introducing an angular dependence on the flux function and solving another approximated equilibrium equation with derivatives with respect to two coordinates and not only one (the radial coordinate) as in this work.

It should be pointed out that some advanced confinement regimes with non inductive currents develop a stable radial hollow current profile, with a central hole where the density is almost zero. On the other hand, a reversed current density with a negative density in the plasma center has not yet been observed.^{3,5,6} However, if the increase in non-inductive current is formed rapidly, the toroidal electric field, transiently negative at the central region, may create a negative central current density.⁶ These scenarios open the possibility of a new class of tokamak configurations, stimulating new theoretical and experimental investigations. In this context, our analytical results may contribute to further investigations on stability and transport in non-nested equilibrium plasma magnetic surfaces.

ACKNOWLEDGMENTS

The authors would like to thank the Brazilian scientific agencies CAPES, CNPq, and FAPESP for the financial support, the referee's suggestions and comments, and the discussions with David Ciro Taborda.

- ¹J. Wesson, *Tokamaks* (Clarendon, Oxford, 1997).
- ²B. C. Stratton, J. A. Breslau, R. V. Budny, S. C. Jardin, W. Park, H. R. Strauss, L. E. Zakharov, B. Alper, V. Drozdov, N. C. Hawkes, S. Reyes-Cortes, and contributors to the EFDA-JET Workprogramme, *Plasma Phys. Controlled Fusion* **44**, 1127 (2002).
- ³N. C. Hawkes, B. C. Stratton, T. Tala, C. D. Challis, G. Conway, R. DeAngelis, C. Giroud, J. Hobirk, E. Joffrin, P. Lomas, P. Lotte, J. Mailloux, D. Mazon, E. Rachlew, S. Reyes-Cortes, E. Solano, and K-D. Zastrow, *Phys. Rev. Lett.* **87**, 115001-1 (2001).
- ⁴A. C. C. Sips, *Plasma Phys. Controlled Fusion* **47**, A19 (2005).
- ⁵T. Fujita, T. Suzuki, T. Oikawa, A. Isayama, T. Hatae, O. Naito, Y. Sakamoto, N. Hayashi, K. Hamamatsu, S. Ide, and H. Takenaga, *Phys. Rev. Lett.* **95**, 075001 (2005).
- ⁶T. Fujita, *Nucl. Fusion* **50**, 113001 (2010).
- ⁷M. S. Chu and P. B. Parks, *Phys. Plasmas* **9**, 5036 (2002).
- ⁸A. A. Martynov, S. Yu Medvedev, and L. Villard, *Phys. Rev. Lett.* **91**, 085004-1 (2003).
- ⁹S. Wang, *Phys. Rev. Lett.* **93**, 155007-1 (2004).
- ¹⁰P. Rodrigues and J. S. Bizarro, *Phys. Rev. Lett.* **95**, 015001-1 (2005).

¹¹P. Rodrigues and J. S. Bizarro, Phys. Rev. Lett. **99**, 125001-1 (2007).

¹²Y. Hu, Phys. Plasmas **15**, 022505 (2008).

¹³M. Y. Kucinski, I. L. Caldas, L. H. A. Monteiro, and V. Okano, J. Plasma Phys. **44**, 303 (1990).

¹⁴E. C. Silva, I. L. Caldas, and R. Viana, IEEE Trans. Plasma Sci. **29**, 617 (2001)

¹⁵M. Roberto, E. C. Silva, I. L. Caldas, and R. L. Viana, Phys. Plasmas **11**, 214 (2004).